Journal of the Ceramic Society of Japan 116 [3] 374-379 2008 Paper

Synthesis of hydrogen and carbon monoxide from methane and carbon dioxide over Ni–Al_2O_3 catalyst

Soichiro SAMESHIMA, Yoshihiro HIRATA, Junya SATO* and Naoki MATSUNAGA*

Department of Advanced Nanostructured Materials Science and Technology, Kagoshima University, 1-21-40, Korimoto, Kagoshima 890-0065
***Department of Applied Chemistry and Chemical Engineering, Kagoshima University, 1-21-40, Korimoto, Kagoshima 890-0065**

The mixed gas of CH_4 (50%) and CO_2 (50%) was fed into the porous compacts of alumina-supported Ni (30 vol%) catalyst heated at 673–973 K. Hydrogen was produced by the reaction of the mixed gas ($CH_4+CO_2 \rightarrow 2CO+2H_2$). A part of produced CO decomposed to CO_2 and C ($2CO \rightarrow CO_2+C$) below 873 K. As a parallel reaction, the decomposition of CH_4 occurred in the wide temperature range from 673–973 K. The carbon deposition suppressed the flow of the outlet gas.

Key-words: Methane, Carbon dioxide, Hydrogen, Carbon monoxide, Biogas, Solid oxide fuel cell, Thermal decomposition

[Received September 11, 2007; Accepted January 17, 2008]

1. Introduction

Solid oxide fuel cell (SOFC) has many advantages such as high energy conversion efficiency, clean product (H_2O), no loss of solid electrolyte and a variety of fuel gases. Rare earth-doped ceria (RDC) is a possible electrolyte for the low temperature SOFC because of its high oxide ion conductivity.[1)–3)] Reducing the operation temperature enhances the thermal stability of electrodes or interconnector and increases the lifetime of SOFC. Furthermore the transference number of oxide ion of RDC approaches unity by 10^{-15} Pa of oxygen partial pressure at 773 K.[4)] Biogas produced from excrement of domestic animals contains 60% of methane, 40% of carbon dioxide and a small amount of H_2S and NH_3.[5),6)] The authors reported that the terminal voltage and electric power density of SOFC with Gd-doped ceria electrolyte (GDC) and Ni (30 vol%)-GDC porous anode were lower for biogas than for H_2 at 1073 K because of a high activation energy of thermal decomposition of CH_4 at a thin anode (thickness $<100\,\mu$m).[7)] When the thickness of Ni (30 vol%)-Al_2O_3 porous compact is increased to 10 mm, pyrolysis of methane started at 673 K. The thickness of the Ni-based anode is a key factor to operate SOFC using biogas. Barnett et al. reported a power density of 370 mW/cm^2 of SOFC using CH_4 fuel at 823 K.[8)] When carbon is deposited on the anode during the supply of methane, the electric power of SOFC decreases. Noble metals (Pt, Pd and Rh) are shown to suppress more the carbon deposition than Ni.[9)] However, CH_4 is reformed with CO_2 to produce H_2 and CO which are used as fuels of SOFC ($CH_4+CO_2 \Leftrightarrow 2H_2+2CO$). This favorable reaction is expected to suppress the carbon deposition from methane. Many papers report CH_4 reforming with CO_2 over Ni/Al_2O_3 catalyst and discuss the reaction mechanisms of the carbon deposition.[10)–12)] Ni, Co and Fe are useful catalyst accelerating the above dry reforming. The hydrogen and carbon monoxide react with O^{2-} ion supplied from RDC electrolyte to form H_2O, CO_2 and electrons. The produced CO_2 is again mixed with biogas to make a closed system of $CO \rightarrow CO_2 \rightarrow CO$. That is, both methane and carbon dioxide of biogas can be used as fuels of SOFC. The above closed system of biogas is useful in producing electric power and in no exhaust of CH_4 and CO_2 into air. Some researchers use alkaline earth oxide or rare-earth oxide as a support material of Ni. These oxides adsorb CO_2 and accelerate the dissociation of CO_2 to CO and O. The formed O and CH_4 adsorbed on Ni react to form CO and H_2.[9)] Cui et al. reported that reaction rate of reforming of CH_4 with CO_2 was dominated by the dissociation rate of CH_4 at low temperatures (<850 K) and by rate of the reaction CHx (adsorbed species derived from CH_4) and CO_2 at a high temperature (<900 K).[13)] Effect of addition of alkaline metal,[10)] noble metal[11)] or rare-earth oxide[12)] to Ni-Al_2O_3 catalyst on carbon deposition has been also investigated. Most of the papers of Ni-Al_2O_3 catalyst treat 5 vol% of Ni but little information on reforming of CH_4 with CO_2 has been reported for anode with high Ni content (30–70 vol%) of SOFC, which has a sufficient electronic conductivity.

This paper reports the basic information of reforming of CH_4 with CO_2 on Al_2O_3-supported 30 vol% of Ni catalyst at 673–973 K to use biogas as a fuel of SOFC in a next stage. The reaction of dry reforming and carbon deposition was discussed on the calculated free energy (ΔG) using the partial pressure of outlet gas.

2. Experimental

Alpha-alumina powder ($Al_2O_3>99.99$ mass%, median size 0.48 μm, Sumitomo Chemical Co., Ltd.) was immersed in a 1.4 mol/l $Ni(NO_3)_2$ solution at a volume ratio of Ni/Al_2O_3 = 30/70. The suspension was freeze-dried and the mixed powders were calcined at 673 K for 1 h in air. The calcined NiO–Al_2O_3 mixed powders were dispersed at 10 vol% solid in double distilled water and consolidated into a columnar shape of 16 mm diameter and 10 mm height by casting in a gypsum mold. The dried compact was calcined at 1073 K for 1 h in air. The calcined NiO–Al_2O_3 compact with 11 mm diameter was set inside of a SiO_2–Al_2O_3 tube and was reduced to Ni by passing 70 vol% H_2–30 vol% Ar gas at 973 K for 10 h.[14)] A mixed gas of $CH_4 : CO_2 = 1 : 1$ volume ratio was fed at 50 ml/min to the Ni–Al_2O_3 compact at 673–973 K. The phases of NiO–Al_2O_3 compact before and after the reduction were identified by X-ray diffraction

(RINT 2200, Rigaku Co., Tokyo). The relative density and porosity of the $NiO-Al_2O_3$ compact were measured by the Archimedes method using distilled water. The microstructure of the sample was observed using scanning electron microscope (SM-300, Topcon Co., Tokyo). The composition of passing gas was analyzed to determine the reforming fraction of methane and carbon dioxide and the amounts of formed hydrogen and carbon monoxide by gas chromatography (GT 3800, Yanaco Co., Kyoto) with molecular sieve 5A and porapack Q using thermal conductivity detector at 393 K. The outlet gas of 0.5 ml was injected into Ar carrier gas at 323 K. The amount of carbon deposition in the $Ni-Al_2O_3$ compact was measured with thermogravimetry and differential thermal analysis (TG-DTA) at a heating rate of 5 K/min up to 1473 K in air at the flow rate of 100 ml/min (Thermoflex, Rigaku Co., Tokyo, Japan). Carbon is burn out as carbon dioxide and Ni is oxidized to NiO.[14] The weight change during the heating is expressed by Eq. (1),

$$\frac{\Delta W}{W_0+W_C}=\frac{(W_{NiO}-W_{Ni})-W_C}{W_0+W_C}$$

$$=\frac{[V_0(1-P)0.3]\left(1-\frac{M_{NiO}}{M_{Ni}}\right)-W_C}{W_0+W_C} \quad (1)$$

where V_0, W_0 and P are the volume of powder, weight and porosity of Ni/Al_2O_3 compact, respectively, W_c, W_{NiO} and W_{Ni} the weight of carbon, NiO and Ni, respectively. The number 0.3 is the volume fraction of Ni in Ni/Al_2O_3 compact, MNiO and MNi are the molecular weight of NiO and Ni.

3. Results and discussion

3.1 Sample preparation

Figure 1 shows the X-ray diffraction patterns of $NiO-Al_2O_3$ compact heated at (a) 1073 K, (b) 1273 K in air, and (c) 973 K in 70 vol% H_2–30 vol% Ar flow. Although no compound was formed at 1073 K, $\alpha-Al_2O_3$ and NiO reacted to form $NiAl_2O_4$ spinel at 1273 K. The $NiO-Al_2O_3$ compact heated in air at 1073 K was reduced to $Ni-Al_2O_3$ in the H_2-rich atmosphere and no reaction occurred between Ni and Al_2O_3. **Table 1** summarizes the relative density and porosity of $NiO-Al_2O_3$ compacts before and after the reaction with CH_4-CO_2 gas. The $NiO-Al_2O_3$ compacts contained 37–61% of open pores and 1–18% of closed pores. The open porosity increased and closed porosity decreased by the reduction of NiO to Ni with H_2 gas. For example, the open and closed porosity of sample No. 1 were 63.5 and 0.1%, respectively, after the reduction with H_2 gas. As seen in Table 1, the open porosity of $Ni-Al_2O_3$ compact was still large after the reforming of CH_4 with CO_2 for 2.1 h at 773 K, 3.2 h at 873 K and 3.8 h at 973 K, respectively. However, the blockage of CH_4-CO_2 gas flow occurred in the reaction system for 0.55–2.35 h as shown in Table 1. This phenomenon is discussed in section 3.4.

3.2 Thermodynamic calculation

Figure 2 shows the standard Gibbs free energy (ΔG°) for Eq. (1) in the $CH_4-CO_2-H_2-CO$ system.

$$CH_4(g)+CO_2(g)\Leftrightarrow 2CO(g)+2H_2(g) \quad (1)$$

The free energy changes to minus values above 915 K. Equations (2) and (3) represent the possible subsequent reactions of formed CO.

$$2CO(g)\Leftrightarrow CO_2(g)+C(s) \quad (2)$$
$$2CO(g)\Leftrightarrow O_2(g)+2C(s) \quad (3)$$

In these reactions, solid carbon is deposited. The free energy for Eq. (2) is negative values at a low temperature below 976 K. On the other hand, the free energy for Eq. (3) is positive values in the wide temperature range of 400–1400 K.

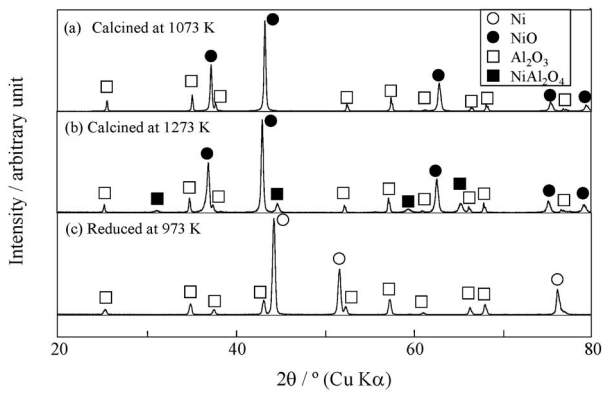

Fig. 1. X-ray diffraction patterns of $NiO-Al_2O_3$ compacts heated at (a) 1073 K, (b) 1273 K in air, and at (c) 973 K in 70 vol% H_2–30 vol% Ar flow.

Table 1. Relative Density and Porosity of $NiO-Al_2O_3$ Compacts before and after Reaction with CH_4-CO_2 Gas. The Calcined $NiO-Al_2O_3$ Compact was Heated at 973 K for 10 h in 70 vol% H_2–30 vol% Ar Gas to form Ni before Reaction with CH_4-CO_2 Gas

Sample	Calcined at 1073 K in air			After reforming of CH_4 *				
No.	Relative density (%)	Open pores (%)	Closed pores (%)	Reaction temperature (K)	Blockage time (h)	Relative density (%)	Open pores (%)	Closed pores (%)
1	39.0	58.4	2.6			–	–	–
2	37.3	61.4	1.3	673	2.35	–	–	–
3	44.2	41.2	14.7	773	0.75	36.2	59.9	3.9
4	44.4	37.3	18.3	873	0.55	37.0	47.9	15.1
5	36.8	50.3	13.0	973	1.72	33.7	57.4	8.8

– : not measured.

* : The density and porosity of $Ni-Al_2O_3$ compact were measured after the reaction for 2.1 h at 773 K, 3.2 h at 873 K and 3.8 h at 973 K (See Fig.8).

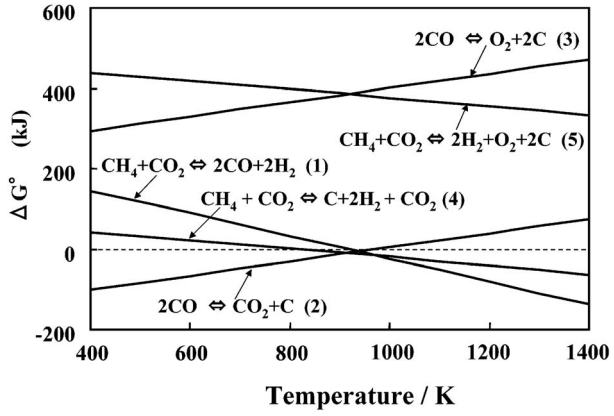

Fig. 2. Standard Gibbs free energy for Eqs. (1)-(5) as a function of temperature.

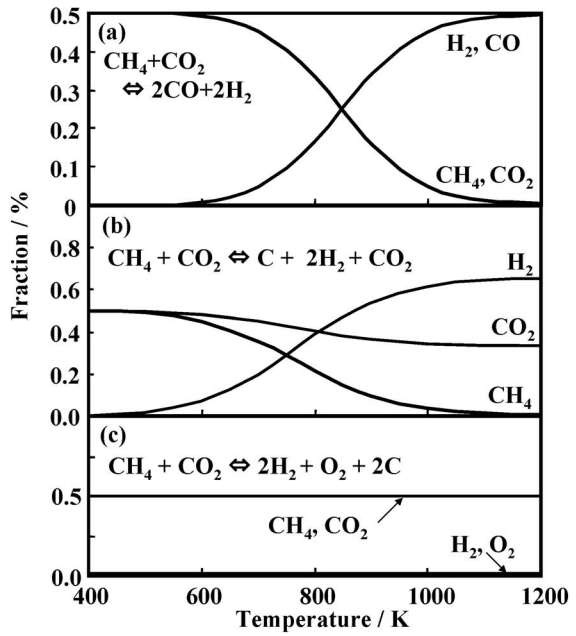

Fig. 3. Fractions of CH_4, CO_2, H_2, CO and O_2 for Eqs. (1), (4) and (5) at an initial pressure of $P_{CH_4}=P_{CO_2}=5\times10^4$ Pa.

The coupling of Eqs. (1) and (2) gives Eq. (4),

$$CH_4(g)+CO_2(g)\Leftrightarrow 2H_2(g)+CO_2(g)+C(s) \quad (4)$$

Equation (4) expresses the decomposition of CH_4 and in CO_2 atmosphere and gives negative values of standard free energy above 800 K. The substitution of Eq. (3) for Eq. (1) yields Eq. (5).

$$CH_4(g)+CO_2(g)\Leftrightarrow 2H_2(g)+O_2(g)+2C(s) \quad (5)$$

The standard free energy for Eq. (5) is positive values in the temperature range from 400 to 1400 K.

Figure 3 shows the fractions of CH_4, CO_2, CO, H_2 and O_2 calculated using the standard free energy for Eqs. (1), (4) and (5) at an initial pressure of $P_{CH_4}=P_{CO_2}=5.0\times10^4$ Pa. The fraction of decomposition of CH_4 by Eq. (1) becomes significant above 600 K and reaches 99% at 1100 K. A similar pyrolyisis characteristic of CH_4 is also calculated for Eq.

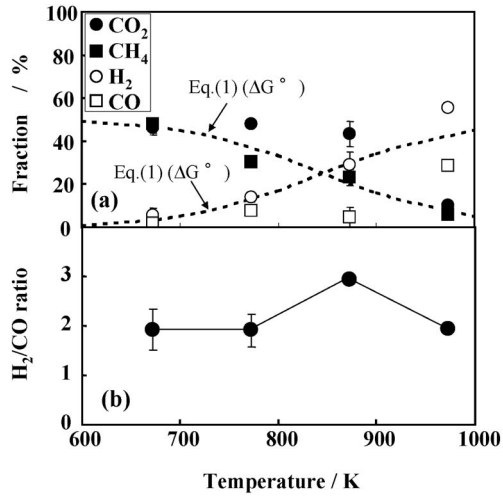

Fig. 4. Fractions of CH_4, CO_2, H_2 and CO (a) and H_2/CO (b) ratio as a function of reaction temperature.

(4). In Eq. (4), CO_2 exists in the wide temperature range. In Eq. (5), no reaction of CH_4 and CO occurs at a given standard free energy.

3.3 Reforming of CH_4 with CO_2

Figure 4(a) shows the fractions of CH_4, CO_2, H_2 and CO as a function of reaction temperature. Solid circles indicate the average fraction for 0.6–2.4 h of reforming of CH_4 where no blockage of passing gas occurred in the Ni-Al_2O_3 compacts. The amounts of CH_4 and CO_2 decreased with increasing temperature, and were close to 6% and 10% at 973 K, respectively. The amount of H_2 formed increased gradually with increasing temperature. The production amount of CO was small and was not sensitive to the reaction temperature. The fractions of CH_4 and CO_2 at 973 K were comparable to the reported values using 3.1–4.8 vol% Ni-Al_2O_3 catalyst under the similar experimental condition in references 10 and 11. The oxygen partial pressure in the outlet gas was independent of reaction time at each reaction temperature and as follows: 4.0×10^{-19} Pa at 673 K, 9.3×10^{-18} Pa at 773 K, 3.6×10^{-16} Pa at 873 K and 5.5×10^{-14} Pa at 973 K. These values were very small as compared with the partial pressures of the other gases. Figure 4(b) shows the H_2/CO ratio as a function of reaction temperature. The average ratio at 673–973 K was in the range from 1.9 to 2.9. These values were higher than the reported value (0.86) in reference 10.

The above results were compared with the fractions calculated from standard free energy (Fig. 3). The dotted lines in Fig. 4 represents the fractions of CH_4 and H_2 based on Eq. (1). The measured fractions of these gases were well fitted by Eq. (1). However, the fractions of CO and CO_2 deviated largely from Eq. (1) at 773–873 K. As reported in the latter section, carbon deposition was observed on Ni/Al_2O_3 compact in the wide temperature range of 673–973 K. This result suggests that Eq. (2) or (3) occurred after the formation of CO. When Eq. (4) was compared with the measured fractions of CH_4 and H_2, no agreement was recognized. This comparison indicates that CO formed by Eq. (1) was not in equilibrium state or steady state with Eq. (2). Therefore, the result in Fig. 4 is interpreted that (1) CH_4 and CO_2 reacted

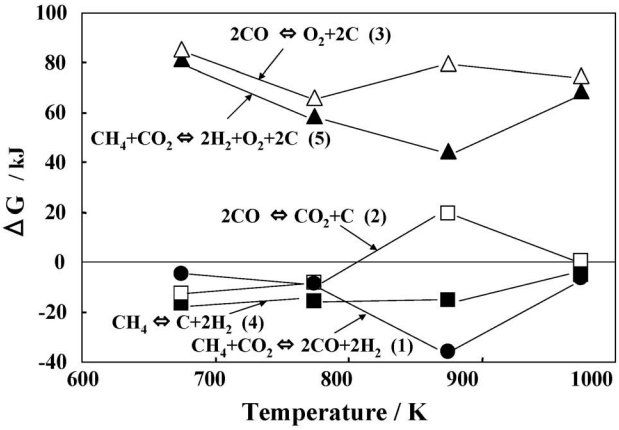

Fig. 5. Change of free energy for Eqs. (1)–(5) calculated from the measured partial pressures of CH_4, CO_2, H_2, CO and O_2.

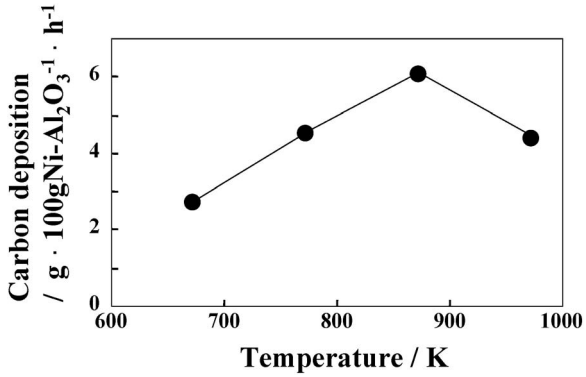

Fig. 6. Carbon deposition on Ni–Al_2O_3 compacts as a function of reaction temperature.

to form CO and H_2, and (2) a part of formed CO molecules decomposed to CO_2 and C. As a result, CO_2 concentration became relatively high and CO concentration was low at 773 and 873 K. The significant decrease of CO_2 fraction and the increased amounts of CO and H_2 at 973 K are not explained by only the decomposition of CH_4 in Fig. 3 (b) or the reaction by Eq. (2), because these reactions are accompanied by the formation of CO_2 in the outlet gas.

Figure 5 shows the change of free energy (ΔG) for Eqs. (1)–(5) calculated from the measured partial pressure of CH_4, CO_2, H_2, CO_2 and O_2. Equation (6) shows the free energy for Eq. (1). A similar equation was used to calculate ΔG value for the other reactions.

$$\Delta G = \Delta G^{\circ} + RT \ln \left[\frac{P_{CO}{}^2 P_{H_2}{}^2}{P_{CH_4} P_{CO_2}} \right] \qquad (6)$$

As seen in Fig. 5, ΔG for Eq. (1) was negative values in the temperature range from 673 to 973 K. This calculation supports that chemical reaction by Eq. (1) proceeded at the given temperature range. The ΔG value for Eq. (2) changes to positive above 873 K. The formed CO decomposes to CO_2 and C at 673 and 773 K. This calculation explains the high CO_2 fraction and the formation of carbon at a low temperature range. The positive ΔG values for Eq. (2) above 873 K indicate that the reaction by Eq. (2) was suppressed at a high temperature range. The negative ΔG values for Eq. (4) indicate that the pyrolysis of methane is possible in the wide temperature range shown in Fig. 5. On the other hand, the ΔG values for Eqs. (3) and (5) resulted in positive values in the temperature range from 673 to 973 K. The reaction expressed by Eqs. (3) and (5) do not proceed in the given gas compositions. From the above calculation, the measured result in Fig. 4 (a) is interpreted as follows. Methane reacted with CO_2 to form CO and H_2. The formed CO decomposed to C and CO_2 below 773 K. As a parallel reaction, thermal decomposition of CH_4 proceeded at 673–973 K.

3.4 Carbon deposition

Carbon deposition over the Ni–Al_2O_3 compact and the inside of the SiO_2–Al_2O_3 tube was observed in all the experiments at 673–973 K. The XRD patterns of Ni–Al_2O_3 compact after the reaction at 873 and 973 K confirmed the formation of graphite at $2\theta = 26.6^{\circ}$ of Cu Kα.[15] The above result is explained by the negative values of ΔG for Eqs. (2) and (4) in Fig. 5. **Figure 6** shows the amount of carbon deposited on Ni–Al_2O_3 compact as a function of reaction temperature. These values in this study were almost close to the previously reported values of 4.7[10] and 2.4[11] g of carbon/100 g of catalyst ·h at 973 and 1073 K, respectively. The formation tendency of carbon with reaction temperature was in accordance with the H_2/CO ratio in Fig. 4 (b). That is, the CO formed by Eq. (1) decomposes to CO_2 and C at the low temperature range. However, this reaction is suppressed above 873 K. The decrease of the amount of carbon at 973 K in Fig. 6 may be related to the above suppression of carbon formation. Another reaction by Eq. (4) contributes to the formation H_2 and C. It is reported that the dissociation of CH_4 is responsible for the carbon deposition on the catalyst above 873 K because of the slow rate of reaction between CH_x (adsorbed species derived from CH_4) and CO_2.[10]

Figure 7 shows the typical microstructure of Ni–Al_2O_3 compact (a) before and (b) after the reaction of CH_4 and CO_2 at 873 K for 3 h. Open pores were observed between Al_2O_3 or Ni grains. After the reaction of CH_4–CO_2 system, the microstructure changed to a dense one. **Figure 8** shows the flow rate of outlet gas during the reaction at 673–973 K. When an alumina compact without Ni was used, the flow rate of the CH_4–CO_2 mixed gas was constant and no carbon was deposited on Al_2O_3 compact after 2 h at 973 K. This result indicates that Ni in the Al_2O_3 compact promotes the reactions by Eqs. (1), (2) and (4). The gradual increase of flow rate with increasing temperature is related to the volume increase of the gases. As seen in Fig. 8, the flow rate of the outlet gas decreased after 0.5 h of reaction time. The blockage of gas flow occurred at 2.35, 0.75, 0.55 and 1.72 h at 673, 773, 873 and 973 K, respectively. This result is associated with the carbon deposition in the Ni–Al_2O_3 compact. The blockage time became shorter when the amount of deposited carbon increased (Fig. 6). **Figure 9** shows the relation between open porosity of starting NiO–Al_2O_3 compact and blockage time during the reforming of CH_4 (See Table 1). The increased open porosity is a favorable to extend the blockage time. A similar tendency was also measured when blockage time was plotted against the open porosity of Ni–Al_2O_3 compact after the reforming of CH_4. Both open porosity and carbon deposition affected the blockage time. The time for no blockage of gas flow was for

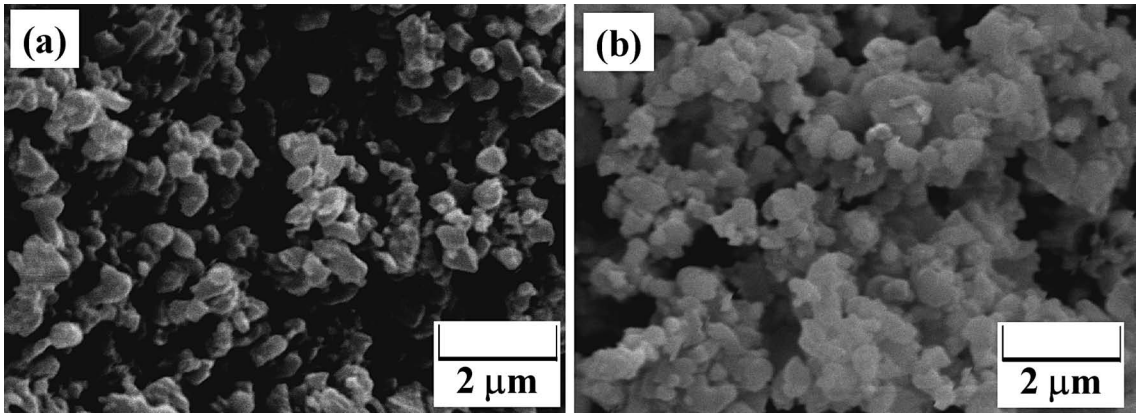

Fig. 7. Microstructures of Ni-Al_2O_3 compacts before (a) and after (b) the reaction of CH_4-CO_2 system at 873 K for 3 h.

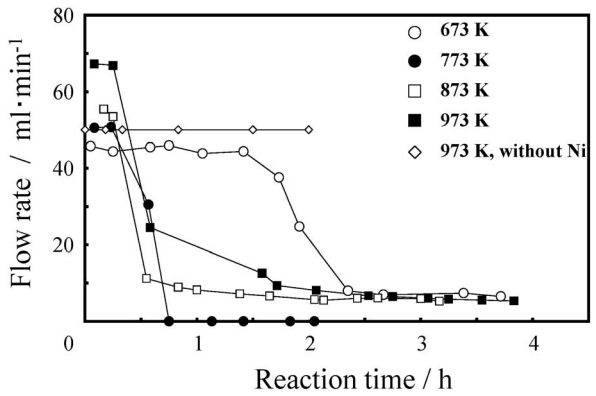

Fig. 8. Flow rate of outlet gas during the reaction at 673–973 K.

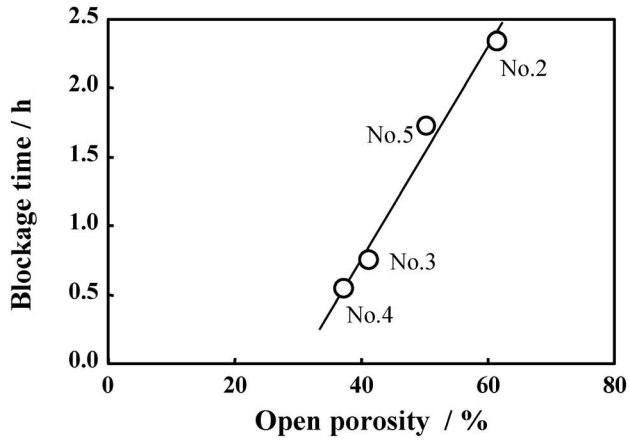

Fig. 9. Relation between open porosity of starting NiO-Al_2O_3 compact and blockage time during the reforming of CH_4 (See Table 1 for samples).

4–40 h in reported papers.[10)–12)] In these papers, sub-millimeter sized powder catalyst was used. However, Ni/Al_2O_3 compact of submicrometer-sized powder was used in present experiment. The difference of blocking time between above two types of catalyst is related to the microstructure of catalyst. On the other hand, No. 3 of Ni-Al_2O_3 compact after the blockage at 773 K contained still 59.9% of open porosity (Table 1). In addition, it was found that the amount of carbon deposited was larger for the upper part of Ni-Al_2O_3 compact than for the lower part against the flow of CH_4-CO_2 gas after the reaction at 1127 K for 2 h. These results suggest the carbon deposition occurred in the upper part of the Ni-Al_2O_3 against CH_4-CO_2 flow and the open porosity of the lower part of the Ni-Al_2O_3 compact was still high. This phenomenon is characterized by the large amount of Ni for electronic conduction of anode in SOFC. It is necessary to control the anode structure in the Ni-Al_2O_3 compact to suppress the blockage at the anode of SOFC with large amount of Ni.

4. Conclusions

(1) Ni in the porous Al_2O_3 compact promoted the reaction of the CH_4-CO_2 system.

(2) CH_4 reacted with CO_2 in the Ni-Al_2O_3 compact to form H_2 and CO above 673 K ($CH_4+CO_2 \rightarrow 2H_2+2CO$).

(3) The formed CO decomposed to CO_2 and C below 873 K. This reaction yielded a relatively high CO_2 concentration and deposition of carbon.

(4) As a parallel reaction, thermal decomposition of CH_4 proceeded to form H_2 and C in the temperature range from 673 to 973 K ($CH_4+ \rightarrow C+2\ H_2$).

(5) Carbon deposition occurred in the upper part of the Ni-Al_2O_3 compact with large amount of Ni for electronic conduction against CH_4-CO_2 gas flow. The blockage time became longer with increasing open porosity of the Ni-Al_2O_3 compact.

References

1) K. Higashi, K. Sonoda, H. Ono, S. Sameshima and Y. Hirata, *J. Mater. Res.*, 14, 957–967 (1999).
2) S. Sameshima, H. Ono, K. Higashi, K. Sonoda, Y. Hirata and Y. Ikuma, *J. Ceram. Soc. Japan*, 108, 1060–1066 (2000).
3) Y. Hirata, S. Yokomine, S. Sameshima, T. Shimonosono, S. Kishi and H. Fukudome, *J. Ceram. Soc. Japan*, 113, 597–604 (2005).
4) T. Shimonosono, Y. Hirata, S. Sameshima and T. Horita, *J. Am. Ceram. Soc.*, 88, 2114–2120 (2005).
5) Y. Lu and L. Shaefer, *J. Power Sources*, 135, 184–191 (2004).
6) M. Nagamori, Y. Hirata and S. Sameshima, *Mater. Sci. Forum*, 544–545, 985–988 (2007).

7) H. Ohshige, Y. Hirata and S. Sameshima, *Adv. Ceram. Proc. Inter.*, 3, 1–4 (2006).
8) E. P. Murray, T. Tsai and S. S. Barnett, *Nature*, 400, 649–651 (1999).
9) K. Tomoshige and K. Fujimoto, *J. Japan Petroleum Institute*, 44, 65–79 (2001) [in Japanese].
10) J. J. Juan, M. C. R. Martinez and M. J. I. Gomez, *Applied Catalysis A: General*, 301, 9–15 (2006).
11) Z. Hou, P. Chen, H. Fang, X. Zheng and T. Yashima, *International J. Hydrogen Energy*, 31, 555–561 (2006).
12) M. Benito, S. Garcia, P. F. Aparicio, L. G. Serrano and L. Daza, *J. Power Sources*, 196, 177–183 (2007).
13) Y. Cui, H. Zhang, H. Xu and W. Li, *Applied Catalysis A: General*, 318, 79–88 (2007).
14) S. Sameshima, Y. Hirata and K. Higashinakagawa, Proceedings of 6th Pacific Rim Conference on Ceramic and Glass Technology, The American Ceramic Society, CDR, 2006.
15) ICCD card No. 75–1621.